

GROWTH OF DUST GRAINS IN A LOW-METALLICITY GAS AND ITS EFFECT ON THE CLOUD FRAGMENTATION

GEN CHIAKI¹, TAKAYA NOZAWA², AND NAOKI YOSHIDA^{1,2}

To Appear in ApJL

ABSTRACT

In a low-metallicity gas, rapid cooling by dust thermal emission is considered to induce cloud fragmentation and play a vital role in the formation of low-mass stars ($\lesssim 1 M_{\odot}$) in metal-poor environments. We investigate how the growth of dust grains through accretion of heavy elements in the gas phase onto grain surfaces alters the thermal evolution and fragmentation properties of a collapsing gas cloud. We calculate directly grain growth and dust emission cooling in a self-consistent manner. We show that MgSiO_3 grains grow sufficiently at gas densities $n_{\text{H}} = 10^{10}$, 10^{12} , and 10^{14} cm^{-3} for metallicities $Z = 10^{-4}$, 10^{-5} , and $10^{-6} Z_{\odot}$, respectively, where the cooling of the collapsing gas cloud is enhanced. The condition for efficient dust cooling is insensitive to the initial condensation factor of pre-existing grains within the realistic range of 0.001–0.1, but sensitive to metallicity. The critical metallicity is $Z_{\text{crit}} \sim 10^{-5.5} Z_{\odot}$ for the initial grain radius $r_{\text{MgSiO}_3,0} \lesssim 0.01 \mu\text{m}$ and $Z_{\text{crit}} \sim 10^{-4.5} Z_{\odot}$ for $r_{\text{MgSiO}_3,0} \gtrsim 0.1 \mu\text{m}$. The formation of a recently discovered low-mass star with extremely low metallicity ($\leq 4.5 \times 10^{-5} Z_{\odot}$) could have been triggered by grain growth.

Subject headings: dust, extinction — galaxies: evolution — ISM: abundances — stars: formation — stars: low-mass — stars: Population II

1. INTRODUCTION

Dust grains in the early universe are considered to be crucial for low-mass star formation in the low-metallicity gas.³ The efficient cooling by dust thermal emission can trigger the fragmentation of the gas at densities $n_{\text{H}} \sim 10^{13}$ – 10^{15} cm^{-3} and gas temperature $T_{\text{g}} \sim 1000 \text{ K}$, where the corresponding Jeans mass is less than one solar mass (Schneider et al. 2003; Omukai et al. 2005). In the early universe, dust grains are considered to be predominantly supplied by core-collapse supernovae; grains are formed in the supernova ejecta (Todini & Ferrara 2001; Nozawa et al. 2003) but a part of them are destroyed by the reverse shock penetrating into the ejecta (Nozawa et al. 2007; Bianchi & Schneider 2007). Thus, the depletion factor of dust, f_{dep} (the mass ratio of dust to metals), is determined by the balance between the formation and destruction of grains.

Schneider et al. (2012) followed the thermal evolution of gas clouds adopting the depletion factors for their models of dust formation and destruction in supernovae. For metallicity Z , the absolute amount of dust is related to the dust-to-gas mass ratio, $\mathcal{D} = f_{\text{dep}}Z$. Schneider et al. (2012) showed that the condition of cloud fragmentation owing to rapid dust cooling is described as the minimal dust-to-gas mass ratio, $\mathcal{D}_{\text{crit}}$, under the assumption that the dust-to-gas mass ratio is constant in the collapsing cloud. However, Nozawa et al. (2012) recently argued that the dust abundance can be increased by the growth of dust grains through accretion of heavy elements in the gas phase onto grain surfaces. They found that the condensation efficiencies (the num-

ber fraction of an element depleted onto grains) of Si- and Fe-grains increase up to unity at gas densities $n_{\text{H}} = 10^{10}$ – 10^{14} cm^{-3} for elemental abundances $[\text{Si}, \text{Fe}/\text{H}] = -5$ to -3 . However, they did not follow the thermal evolution of the gas clouds to determine whether the conditions for fragmentation are met in the clouds. In this Letter, we investigate the effects of grain growth on the thermal evolution of star-forming clouds by calculating grain growth, formation of hydrogen molecules on the grain surfaces, and dust cooling self-consistently. Then, by investigating possible range of metallicities and initial condensation efficiency factors, we can determine the critical metallicity, the minimal metallicity required for the formation of low-mass fragments.

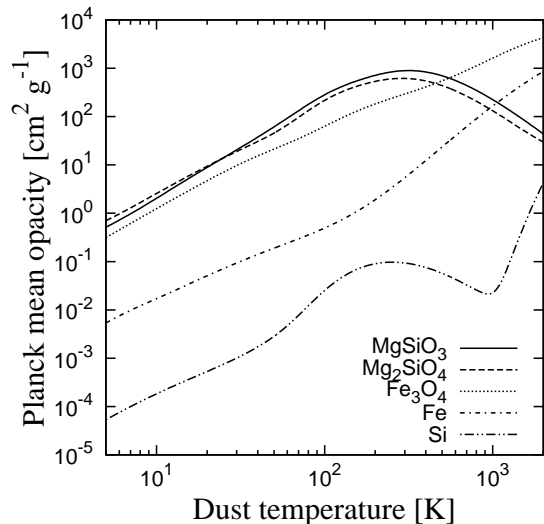


FIG. 1.— Planck mean opacities per unit dust mass for MgSiO_3 (solid), Mg_2SiO_4 (dashed), Fe_3O_4 (dotted), Fe (dot-dashed), and Si (dot-dot-dashed) as a function of dust temperature for a grain radius $0.01 \mu\text{m}$. The values are insensitive to the grain radius except for Fe and Fe_3O_4 .

¹ Department of Physics, Graduate School of Science, University of Tokyo, 7-3-1 Hongo, Bunkyo, Tokyo 113-0033, Japan

² Kavli Institute for the Physics and Mathematics of the Universe (WPI), Todai Institutes for Advanced Study, The University of Tokyo, Kashiwa, Chiba 277-8583, Japan

³ In this Letter, we use the term low-mass for a mass less than $1 M_{\odot}$.

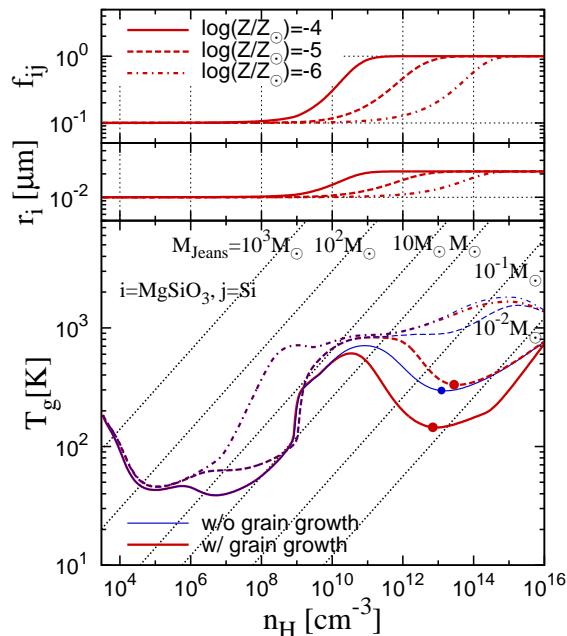


FIG. 2.— Condensation efficiency (top) and the radius of MgSiO_3 grains (middle), and gas temperature (bottom) as a function of hydrogen number density in gas clouds with metallicities $10^{-4} Z_\odot$ (solid), $10^{-5} Z_\odot$ (dotted), and $10^{-6} Z_\odot$ (dot-dashed) for the initial condensation factor 0.1 and the initial grain radius $0.01 \mu\text{m}$. With (red) and without (blue) grain growth. Filled circles mark the states where the fragmentation conditions are met (see the text).

2. NUMERICAL METHOD

We explore the thermal evolution of a collapsing gas cloud with metallicities of $Z = 10^{-6} - 10^{-3} Z_\odot$. The evolutions of density ρ and gas temperature T_g of the cloud core are followed by a one-zone model. Our calculations include chemical reactions of gas species and radiative transfer for line emissions from the gas, and continuum emissions from the gas and dust (see Chiaki et al. 2013, for details).

In our calculations where the growth of dust grains is included, the mass density of dust ρ_d increases with time. Thus, we calculate the continuum optical depth as follows;

$$\tau_{\text{cont}} = (\kappa_g \rho_g + \kappa_d \rho_d) l_{\text{BE}}, \quad (1)$$

where κ_g and κ_d denote the Planck mean opacities of gas and dust, respectively,⁴ ρ_g denotes the mass densities of gas ($\rho = \rho_g + \rho_d$) and l_{BE} is the Bonnor-Ebert length as the typical size of the cloud. Planck-mean opacities of dust κ_d are calculated using optical constants from references tabulated in Nozawa et al. (2008) and shown in Figure 1 for grain species considered in this study. We then obtain the escape fraction of continuum emission as $\beta_{\text{cont}} = \min\{1, \tau_{\text{cont}}^{-2}\}$ (Omukai 2000).

In this study, we primarily consider the growth of MgSiO_3 grains; Mg-silicate is one of the major grain species ejected by core-collapse supernovae (Bianchi & Schneider 2007; Nozawa et al. 2007). We also investigate the growth of Mg_2SiO_4 grains and its

⁴ We should note that here the definition of dust Planck mean opacity κ_d is different from that of κ_{gr} in Omukai (2000) in that the former is defined as the absorption cross section per unit dust mass, while the latter is defined as the absorption cross section per unit gas and dust mass.

effects on the thermal evolution of the gas clouds (see Section 4 below). We assume that the growth of these multi-element grains is regulated by the least abundant gaseous species among reactants, which we call the key element hereafter (see Hirashita & Kuo 2011).

Using the concept of the key element, we calculate grain growth by following the prescription in Nozawa et al. (2012). On the assumption that pre-existing dust grains are spherical with a single initial radius $r_{i,0}$, the evolution of grain radius, r_i , is described by

$$\frac{dr_i}{dt} = s_i \left(\frac{4\pi}{3} a_{i,0}^3 \right) \left(\frac{kT_g}{2\pi m_j} \right)^{1/2} n_j^{\text{gas}}(t), \quad (2)$$

where s_i denotes the sticking probability of the gaseous atoms incident onto grain surfaces, $a_{i,0}$ are the average radius of a monomer molecule in the dust phase *per key element*, and m_j and n_j^{gas} are the mass and the number density of key element j , respectively. In equation (2), the evaporation term can be neglected. When the cloud fragmentation is triggered through efficient cooling by dust, the temperature of dust increases only up to several hundred kelvin, well below the sublimation temperature of MgSiO_3 (~ 1000 K under the condition considered here). Therefore, dust evaporation does not affect the fragmentation condition in the situations we investigate.

The time evolution of condensation efficiency f_{ij} , defined as the number fraction of the key element j locked in grain species i , is described by $f_{ij}(t) = f_{ij,0} [r_i(t)/r_{i,0}]^3$, where $f_{ij,0}$ represents the initial condensation factor. Then, the mass density of the grains is given by $\rho_{d,i}(t) = \rho X_{\text{H}} A_j f_{ij} \mu_i$, where X_{H} is the mass fraction of hydrogen nuclei (set 0.76 here), and μ_i is the molecular weight of grains per key element.

We set the initial density and temperature of a gas cloud to be $n_{\text{H},0} = 3000 \text{ cm}^{-3}$ and $T_{g,0} = 200$ K, respectively.⁵ The initial number fractions of chemical species relative to hydrogen nuclei are $A_e = 10^{-5}$, $A_{\text{D}} = 2.87 \times 10^{-5}$, $A_{\text{H}_2} = 10^{-3}$, $A_{\text{HD}} = 10^{-6}$, irrespective of the metallicity Z . The number abundance of an element j is given as $A_j = A_{j,\odot} (Z/Z_\odot)$, where the solar number abundances of heavy elements, $A_{j,\odot}$, are taken from Caffau et al. (2011a).

The average radius of an atom per key element in the dust phase is taken from (Nozawa et al. 2003), and the sticking coefficient is assumed to be unity. For the scaled solar elemental abundances ($A_{\text{Mg}}/A_{\text{Si}} > 1$), the key element of MgSiO_3 is Si, whose initial condensation factor is taken as $f_{\text{MgSiO}_3, \text{Si},0} = 0.001, 0.01, \text{ and } 0.1$. As for the initial radius of pre-existing grains, we consider four cases of $r_{\text{MgSiO}_3,0} = 0.001, 0.01, 0.1, \text{ and } 1 \mu\text{m}$. Dust temperature is calculated from the balance equation between heating due to collisions with the gas and cooling by dust thermal emission. Also, the formation rate of hydrogen molecules on grain surfaces is calculated by considering impact of hydrogen atoms onto grain surfaces as in Schneider et al. (2006).

⁵ The initial condition of the gas cloud is taken from the values when a supernova shell becomes gravitationally unstable in our one-dimensional calculations of a supernova remnant (Chiaki et al. 2013). We have confirmed that the evolutions of collapsing gas clouds at $n_{\text{H}} > 10^8 \text{ cm}^{-3}$ are insensitive to these initial values.

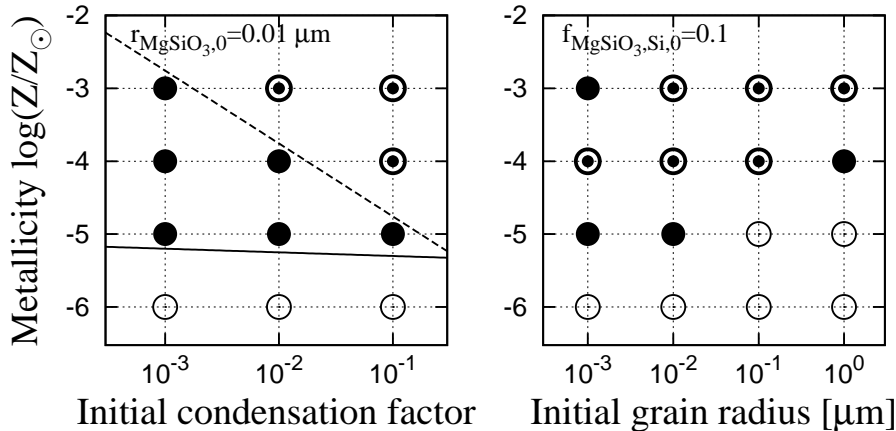


FIG. 3.— Fragmentation properties of the collapsing gas clouds for each model on Z - $f_{\text{MgSiO}_3, \text{Si}, 0}$ (left) and Z - $r_{\text{MgSiO}_3, 0}$ (right) planes. For models marked by double circles, the fragmentation conditions are met both with and without grain growth. While, for models marked by filled circles, the conditions are met only with grain growth. For models marked with open circles, the conditions are not met both with and without grain growth. In left panel, the dashed line shows the metallicity corresponding to the critical dust-to-gas mass ratio given by Schneider et al. (2012) (see the text) and the solid line shows the critical metallicities obtained by detailed calculations.

3. RESULTS

Figure 2 shows the evolutions of the condensation efficiency $f_{\text{MgSiO}_3, \text{Si}}(t)$, the radius $r_{\text{MgSiO}_3}(t)$, and the gas temperature T_g for the initial condensation factor $f_{\text{MgSiO}_3, \text{Si}, 0} = 0.1$ and the initial grain radius $r_{\text{MgSiO}_3, 0} = 0.01 \mu\text{m}$ in gas clouds with metallicities 10^{-6} – $10^{-4} Z_\odot$. For the models with grain growth, the condensation efficiency (mass density of grains) increases at $n_{\text{H}} = 10^{10}$, 10^{12} , and 10^{14}cm^{-3} for $Z = 10^{-4}$, 10^{-5} , and $10^{-6} Z_\odot$, respectively. It eventually converges to unity regardless of metallicities. This is because the timescale characterizing grain growth eventually becomes smaller than the timescale characterizing the free-fall collapse (see Nozawa et al. 2012). The grain radius also reaches to a single value $r_{\text{MgSiO}_3, 0}(1/f_{\text{MgSiO}_3, \text{Si}, 0})^{1/3}$. Since the increase in grain mass density causes enhanced dust cooling, the models with grain growth lead to lower gas temperatures than the models in which the condensation efficiency is constant (i.e., without grain growth).

The circles in Figure 2 depict the phase (on each trajectory) where the cloud is expected to fragment (see Schneider & Omukai 2010, for the detailed description of the criterion for fragmentation). Interestingly, for $Z = 10^{-5} Z_\odot$, the trajectory reaches this phase with grain growth, whereas, without grain growth, the trajectory does not. We therefore conclude that grain growth can reduce the metallicity (Si abundance) above which low-mass fragments can form.

3.1. Critical Metal Abundance

Figure 3 shows fragmentation properties for each model we investigate. The double and filled circles depict the models for which the fragmentation conditions are met when we consider grain growth, and double circles depict the models for which the conditions are met without grain growth. From these results, we can discuss the critical condition for the formation of low-mass fragments.

First, we make the comparison of our results without grain growth with previous works. As the minimal condition of fragmentation, Schneider et al. (2012) found

the critical dust-to-gas mass ratio $\mathcal{D}_{\text{crit}} = 4.4 \times 10^{-9}$ ($= f_{\text{dep}} Z$), above which the dust-induced fragmentation occurs. In the dust model they used, the grains have size distribution functions with the peak at $0.01 \mu\text{m}$. Thus, we can compare their result with our models for $r_{\text{MgSiO}_3, 0} = 0.01 \mu\text{m}$. To apply this, we should convert $f_{\text{MgSiO}_3, \text{Si}, 0}$ into f_{dep} as

$$f_{\text{dep}} = \frac{\rho_{\text{d}, \text{MgSiO}_3}}{\rho_{\text{metal}}} = \frac{X_{\text{H}} A_{\text{Si}} \mu_{\text{MgSiO}_3}}{Z} f_{\text{MgSiO}_3, \text{Si}, 0}, \quad (3)$$

where ρ_{metal} is the mass density of metal in both gas and dust phase and $\mu_{\text{MgSiO}_3} = 100$. With the solar metallicity $Z_\odot = 0.0153$ (Caffau et al. 2011b), we obtain $f_{\text{dep}} = 0.16 f_{\text{MgSiO}_3, \text{Si}, 0}$. In Figure 3, we plot $Z = \mathcal{D}_{\text{crit}} / (0.16 f_{\text{MgSiO}_3, \text{Si}, 0})$ by the dashed line. Our results are consistent with the critical dust-to-gas mass ratio found by Schneider et al. (2012).

Then, we discuss how the critical condition is changed if we consider grain growth. The solid line in Figure 3 shows the critical line above which the fragmentation condition is met with grain growth. Comparison of the two critical lines (solid and dashed line) shows that lower metallicity is generally allowed for low-mass fragment to form when we consider grain growth. Also, the solid line in Figure 3 shows that the critical metallicity is insensitive to the initial condensation factor. This is because even if the initial condensation factor is small ($f_{\text{MgSiO}_3, \text{Si}, 0} \sim 0.001$), the grains grow up to unity before the dust emission cooling becomes effective unless the metallicity is too small.

Instead of the condensation efficiency (dust-to-gas mass ratio), the critical condition is determined by the metallicity and dust size. The estimated critical metallicity is $Z_{\text{crit}} \simeq 10^{-5.5} Z_\odot$ for the initial radius of MgSiO_3 grains $r_{\text{MgSiO}_3, 0} \leq 0.01 \mu\text{m}$, and $Z_{\text{crit}} \sim 10^{-4.5} Z_\odot$ for $f_{\text{MgSiO}_3, \text{Si}, 0} \geq 0.1 \mu\text{m}$. For larger initial radius, the gas density at which grains grow is higher because the total surface area of dust particles, which determines the growth rate, is proportional to r_i^{-1} (for a fixed mass density of dust). The right panel of Figure 3 shows that for $r_{\text{MgSiO}_3, 0} = 0.001$ and $Z = 10^{-3} Z_\odot$, the fragmentation conditions are not met without grain growth, since heat-

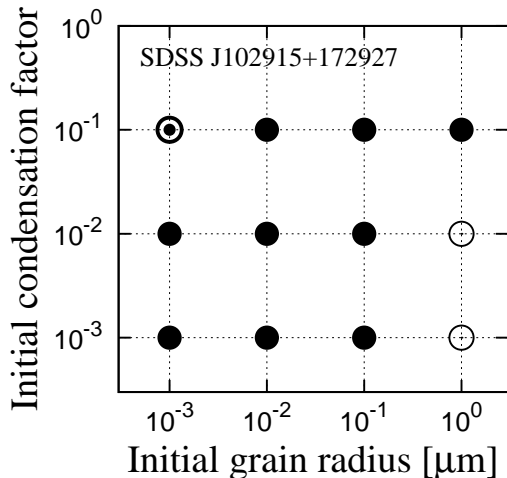


FIG. 4.— Fragmentation conditions of collapsing gas clouds on $f_{\text{MgSiO}_3, \text{Mg}, 0} - r_{\text{MgSiO}_3, 0}$ plane for the abundance of heavy elements of SDSS J102915+172927. Symbols represents the same meaning as Figure 3.

ing due to H_2 formation compensates for cooling by dust emission.

3.2. Application to SDSS J102915+172927

We perform the calculations of grain growth and evolution of collapsing gas, adopting the abundance of heavy elements for the star SDSS J102915+172927: $A_{\text{C}} = 1.58 \times 10^{-8}$, $A_{\text{O}} = 2.51 \times 10^{-8}$, $A_{\text{Mg}} = 8.91 \times 10^{-10}$, $A_{\text{Si}} = 1.78 \times 10^{-9}$, and $A_{\text{Fe}} = 3.39 \times 10^{-10}$, corresponding to the metallicity $4.5 \times 10^{-5} Z_{\odot}$. Note that the abundance of carbon is an upper limit because no strong carbon enhancement is evident in the stellar spectrum. Also, they estimate the oxygen abundance, assuming the typical excess of the α -element oxygen (Caffau et al. 2011a). Given the abundance of the gas, we aim at constraining the initial condensation factor and the initial grain radius necessary for triggering the formation of the low-mass star.

Figure 4 shows the results of calculations with the growth of MgSiO_3 grains. In the present case, the key element is Mg because of $A_{\text{Mg}}/A_{\text{Si}} < 1$. Interestingly, for most of the cases considered here (all cases except for $f_{\text{MgSiO}_3, \text{Mg}, 0} = 0.01$ and 0.001 with $r_{\text{MgSiO}_3, 0} = 1 \mu\text{m}$), the fragmentation conditions are met. Thus, we argue that the parent cloud of SDSS J102915+172927 could have been enriched with relatively small grains ($r_{\text{MgSiO}_3, 0} \lesssim 0.1 \mu\text{m}$) or otherwise with relatively high condensation factor of dust ($f_{\text{MgSiO}_3, \text{Mg}, 0} \gtrsim 0.1$).

It is worth mentioning that the above results are approximately consistent with those obtained with the scaled solar composition (Figure 3), although the abundance pattern is different. The results for $r_{\text{MgSiO}_3, 0} = 0.01 \mu\text{m}$ in Figure 4 lie between those with metallicity $\log(Z/Z_{\odot}) = -5$ and -4 in the left panel of Figure 3, and the results for $f_{\text{MgSiO}_3, \text{Mg}, 0} = 0.1$ lie between those with metallicity $\log(Z/Z_{\odot}) = -5$ and -4 in the right panel of Figure 3.

4. DISCUSSION

In our calculations for the scaled solar abundances, the least abundant element, silicon, regulates the growth of MgSiO_3 grains. Though we have assumed that Si atoms

are directly accreted onto the grains, a part of or all the Si atoms might be in the form of SiO molecules in dense clouds. We also examine a model in which all Si atoms are in the form of SiO molecules initially. As a result, the density at which grains grow rapidly and the resulting critical metallicity are not changed from the results of models in which we consider Si atoms as the key element.

We also examine the growth of other grain species and the effect of each species on the thermal evolution of clouds. We find that, for the scaled solar composition ($A_{\text{Si}}/A_{\text{Fe}} = 1$), Fe_3O_4 grains grow more slowly than MgSiO_3 , and the gas density at which the condensation efficiency of Fe_3O_4 grains becomes 0.5 is higher than for MgSiO_3 by a factor of ~ 5 . This is because the volume of a monomer of Fe_3O_4 grains ($\propto a_{\text{Fe}_3\text{O}_4, 0}^3$) is smaller than MgSiO_3 and thus the rate of grain growth is smaller (see Equation 2). This is also true for Mg_2SiO_4 grains for which the volume per key element, Mg atom, is smaller than for MgSiO_3 . However, for these grain species, the critical metallicity is the same as for MgSiO_3 grains since these grain species have similar mean opacities (Figure 1) and thus similar cooling efficiencies through thermal emission.

On the other hand, Si grains have mean opacity smaller than MgSiO_3 by orders of magnitude (Figure 1). Thus, even if the condensation efficiency reaches unity, the gas cloud cannot cool down enough to meet the fragmentation conditions even for metallicities $Z \simeq 10^{-2} Z_{\odot}$. The growth of Fe grains results in larger critical abundance than MgSiO_3 because the species also have smaller opacity than MgSiO_3 . Hence, these grain species are unlikely to affect heavily the evolution of clouds. Indeed, Si and Fe grains could be rapidly oxidized into silicate and magnetite in a gas cloud with oxygen-rich composition. Supernova models (N. Tominaga et al. 2013, in preparation) and observations in the Galactic halo (Yong et al. 2012) have suggested that the abundances of oxygen in metal-poor stars are usually $A_{\text{O}}/A_{\text{X}} > 10$ where $X = \text{Mg}, \text{Si}, \text{and Fe}$.

It is considered that C grains might have also large effects on the evolution of collapsing clouds. Yet, it is uncertain whether C grains can grow sufficiently in the collapsing gas because a large fraction of carbon atoms are expected to be locked in CO molecules and are not available for the growth of C grains (Nozawa et al. 2012). Even if CO molecules are accreted onto dust nuclei, the CO ice mantle would be easily evaporated because of its low sublimation temperature. Nevertheless, if the initial condensation factor of C grains is high enough, the cooling of the gas by carbon dust thermal emission may have an impact on the cloud evolution.

We have examined the effect of growth of an individual dust species on collapsing gas clouds separately. In a low-metallicity gas, multiple dust species would grow simultaneously, and thus their combined effects could reduce further the critical metallicity. Dust formation calculations in primordial supernovae (e.g., Todini & Ferrara 2001; Nozawa et al. 2003; Schneider et al. 2006; Bianchi & Schneider 2007) showed that various grains species can be produced. It is important to study how the growth of multiple species of dust affects the thermal evolution of collapsing gas clouds

based on the realistic supernova dust models.

Finally, we have set the sticking probability $s_i = 1$ in the calculations. As seen from Equation (2), a lower sticking probability leads to a lower growth rate of dust. We perform another calculations, setting $s_i = 0.1$. As a result, the fragmentation fails for $Z = 10^{-5} Z_{\odot}$ and $r_{\text{MgSiO}_3,0} = 0.01 \mu\text{m}$. However, even for $s_i = 0.1$, grains with $r_{\text{MgSiO}_3,0} = 0.001 \mu\text{m}$ rapidly grow to cause the cloud fragmentation. We have considered dust grains with a single initial size, but dust grains that were formed and processed in supernovae may have size distribution. Since smaller grains grow more rapidly, the lower limit of size distribution and the initial mass fraction of the small

grains could be crucial quantities for cloud fragmentation. We will investigate these effects comprehensively in our future work.

We thank K. Omukai, R. Schneider, N. Tominaga, and Beate Patzer for fruitful discussion. This work is supported in part by the Grants-in-Aid for Young Scientists (S: 20674003, A: 22684004) and for General Scientists (S: 23224004) by the Japan Society for the Promotion of Science. N.Y. acknowledges financial support from World Premier International Research Center Initiative (WPI Initiative), MEXT, Japan.

REFERENCES

- Bianchi, S., & Schneider, R. 2007, *MNRAS*, 378, 973
 Caffau, E., Bonifacio, P., François, P., et al. 2011b, *Nature*, 477, 67
 Caffau, E., Ludwig, H. G., Steffen, M., Freytag, B., & Bonifacio, P. 2011a, *Sol. Phys.*, 268, 255
 Chiaki, G., Yoshida, N., & Kitayama, T. 2013, *ApJ*, 762, 50
 Hirashita, H., & Kuo, T.-M. 2011, *MNRAS*, 416, 1340
 Nozawa, T., Kozasa, T., Habe, A., et al. 2007, *ApJ*, 666, 955
 Nozawa, T., Kozasa, T., & Nomoto, K. 2012, *ApJ*, 756, L35
 Nozawa, T., Kozasa, T., Tominaga, N., et al. 2008, *ApJ*, 684, 1343
 Nozawa, T., Kozasa, T., Umeda, H., Maeda, K., & Nomoto, K. 2003, *ApJ*, 598, 785
 Omukai, K. 2000, *ApJ*, 534, 809
 Omukai, K., Tsuribe, T., Schneider, R., & Ferrara, A. 2005, *ApJ*, 626, 627
 Schneider, R., Ferrara, A., Salvaterra, R., Omukai, K., & Bromm, V. 2003, *Nature*, 422, 869
 Schneider, R., & Omukai, K. 2010, *MNRAS*, 402, 429
 Schneider, R., Omukai, K., Bianchi, S., & Valiante, R. 2012, *MNRAS*, 419, 1566
 Schneider, R., Omukai, K., Inoue, A. K., & Ferrara, A. 2006, *MNRAS*, 369, 1437
 Todini, P., & Ferrara, A. 2001, *MNRAS*, 325, 726
 Yong, D., Carney, B. W., & Friel, E. D. 2012, *AJ*, 144, 95